Sensors & Actuators: B. Chemical 449 (2026) 139037

Contents lists available at ScienceDirect

Sensors and Actuators: B. Chemical

journal homepage: www.elsevier.com/locate/snb

EGFET-based detection of airborne *E. coli* using a recirculating wetted wall cyclone collection

Soohwan Kim [a,1], Noah Baughman [b,1], Mohamed Badawy [a,e,1], Margaret Armstrong [c], Kristina Wayne [c], Eric Vogel [b], Craig R. Forest [a], David L. Hu [a,d,*], Michael L. Farrell [c]

[a] George W. Woodruff School of Mechanical Engineering, Georgia Institute of Technology, United States of America
[b] School of Materials Science and Engineering, Georgia Institute of Technology, United States of America
[c] Advanced Concepts Laboratory, Georgia Tech Research Institute, United States of America
[d] School of Biological Science, Georgia Institute of Technology, United States of America
[e] Department of Mechanical Design and Production, Faculty of Engineering, Cairo University, Egypt

ARTICLE INFO

Keywords:
Bioaerosol
E. coli
HVAC
Cyclone
EGFET

ABSTRACT

We developed a high-volume bioaerosol collection and analysis prototype device to detect low concentrations of airborne *E. Coli* in 50 minutes. Potential applications of this system include integration into a building's heating, ventilation, and air conditioning system for indoor detection and identification of viral, bacterial, and fungal biological threats. A scaled-down version has potential surveillance use by the military for defense against biological weapons. Our device integrates an array of technologies including (1) the collection of airborne biological particles using a wetted wall cyclone at up to 1200 liters of air per minute, (2) microfluidic particle filtration and concentration, and (3) the extended-gate field-effect transistor (EGFET), which detects both viable and non-viable cells, as the biosensor for target pathogens. The 50-minute operation includes a 12-minute collection phase (8-minutes without recirculation, 3 minutes with recirculation, and 1 minute of residual collection without aerosol input) followed by an 8-minute concentration and a 30-minute detection phase. Using aerosolized particles containing target *Escherichia coli*, we detected concentrations as low as 7.6 colony-forming units (CFU) per liter of air with a sensor surface potential shift of 165 ± 73 mV.

1. Introduction

Airborne transmission of pathogens has long been recognized as a significant vector of infectious diseases such as COVID-19, influenza, and tuberculosis. Tuberculosis (TB) alone caused an estimated 1.6 million deaths in 2021 [1]. These diseases, and many others, are spread from person to person by aerosolized infectious particulates usually expunged from the upper respiratory tract through breathing, talking, singing, coughing, sneezing, etc., especially in confined indoor spaces. A bioaerosol is broadly defined as airborne particles of biological origin, including microorganisms such as bacteria and viruses, as well as non-living materials or compounds derived from plants and animals [2]. In settings as varied as hospitals, offices, and public transit systems, bioaerosol surveillance that can trigger automated air handling control measures could aid in reducing the indoor transmission rates of various infections, thereby improving public health [3]. The World Health Organization (WHO) guideline of 0.5 CFU/L applies specifically to fungal bioaerosols [4,5], yet microbial concentrations in contaminated indoor air have been reported as high as 10^3 CFU/L [6]. Acceptable total bacterial bioaerosol concentrations vary globally, but upper limits are generally in the range of 4.5–10 CFU/L [7]. Reported background levels typically range from 0.02 to 2.6 CFU/L in day-care centers, building interiors, and classrooms [8,9]. In hospital settings, values of 0.02–1.5 CFU/L are commonly reported [10].

Bioaerosol monitoring is needed to address threats to public health by natural or man-made bioaerosol pathogens, and this requires a suitable collection method [11]. In this study, we use wetted wall cyclones, which can sample large volumes of air and transition the target particles into a liquid solution amenable to biological analysis [12]. Recent studies have aimed to integrate various collection techniques into a singular platform for more effective bioaerosol monitoring [2,13], but most are still in the early phases of development and have not yet reached a satisfactory level of integration or efficiency [14]. Devices integrating impactors or electrostatic precipitators for particle collection have been deployed but tend to be bulky, with power consumption and

* Corresponding author at: George W. Woodruff School of Mechanical Engineering, Georgia Institute of Technology, United States of America.
E-mail address: hu@me.gatech.edu (D.L. Hu).
[1] The authors contributed equally.

https://doi.org/10.1016/j.snb.2025.139037
Received 9 July 2025; Received in revised form 21 October 2025; Accepted 27 October 2025
Available online 5 November 2025

sensitivity issues [15–17]. Additionally, filter-based impaction methods require extracting the captured particulate from the filter material for further analysis, making them unsuitable for continuous, real-time monitoring.

In our study, we employ an extended-gate field-effect transistor (EGFET), which has demonstrated high sensitivity for diverse targets such as SARS-CoV-2 antigen, Staphylococcus epidermidis, and pathogen RNA, while also offering cost-effective accessibility [18,19]. Several approaches have been attempted for real-time or near-real-time detection of bioaerosols. Techniques such as Polymerase Chain Reaction (PCR) and immunoassays are frequently employed, but they require a discontinuous centralized laboratory setting. Optical methods, including laser-induced fluorescence [20], Raman scattering [21], and bioluminescence of flexible biosensor film [22,23] have also been considered for rapid detection. These methods are promising in terms of speed and sensitivity but often struggle with the selectivity and specificity required for reliable pathogen detection [24]. SPR is frequently employed as a sensing modality, but EGFET provides a more cost-effective and accessible alternative. By relying on a simple gold surface that can be interfaced with commercial components, EGFET avoids the need for custom fiber SPR sensors, nanoparticle amplification, or tracer-based complexity [25,26].

Many researchers have successfully paired wetted wall cyclones with a sensing element; we briefly review these approaches and compare ours here. Skládal et al. demonstrated *Escherichia coli* (*E. coli*) sensing in aerosols as low as 150 CFU/L by combining a wet cyclone with a potentiometric immunosensing element, immunoSMART [27]. Jiang et al. demonstrated detection of viral particles by combining a cyclone with a custom fiber-optic sensor [28]. Lee et al. utilized DC impedance to detect *E. coli* captured by a wet cyclone [29]. Other highly novel, innovative biosensing techniques have been used alongside cyclone collection. A wet cyclone coupled with an FET-based biosensor has been reported conceptually, but not tested with *E. coli* [30]. Cho et al. demonstrated *E. coli* sensing using a rolling bioluminescent film that enables long term continuous sensing [23]. Puthussery et al. presented a COVID-19 aerosol sensor that integrates a microimmunoelectrode (MIE) with a wet cyclone air sampler [31].

We build upon this body of work to present an accessible and portable sensing system capable of detecting *E. coli* in low-concentration bioaerosols. The EGFET is chosen as the biosensing technique due to its relative ease of access and broad availability. While SPR techniques have proven reliable in the literature, SPR is generally more expensive than EGFETs, which can limit application. Other innovative, bespoke solutions show promise in the literature, such as bioluminescent film and MIE biosensors. However, as relatively niche biosensing techniques the lack of commercial components may limit access for scaling the technology. In addition to the accessibility benefits, this work also builds upon the literature to assess device performance under varying analyte concentration and without requiring amplification or additional sample processing post-filtration.

This study aims to develop an integrated system for the detection of airborne pathogens. We integrated a wetted wall cyclone particle collector, membrane filtration/concentration, and EGFET sensor into a single prototype (Fig. 1). To assist troubleshooting during testing, concentrated samples were manually transferred to the EGFET sensor immediately without additional processing. With suitable modifications to the cyclone and filtration system, future designs could directly integrate the EGFET sensor to enable fully automated capture and detection. Aerosolized *E. coli* was used as a surrogate pathogen to test the efficacy of the system. The use of a wetted wall cyclone allows for the efficient and rapid collection of high volumes of air, which is crucial for detecting low concentrations of pathogens, and we also introduced a novel recirculation mechanism to concentrate the collected hydrosol for improved downstream sensitivity. The microfluidic particle filtration and concentration further enhance the sensitivity of the system by eliminating non-target particles and concentrating the target pathogens, and in contrast to previous work [32], we updated this module with automated peristaltic pumps to precisely control dual-filter operation. Finally, the EGFET enables highly sensitive detection of pathogens by measuring surface potential shifts. This combination significantly reduces detection time and improves accuracy compared to existing systems, which often rely on slower and less sensitive methods.

2. Methods

Below we outline the operation of our integrated particle detection system. Additional details on construction and procedure are available in the supplement.

2.1. Particle collection

Merging the principles of cyclonic separation with wet walls, the wetted wall cyclone (WWC) presents a robust solution to some challenges posed by other airborne particle collection methods such as filtration, impaction, impingement, electrostatic precipitation, and condensation. A strength of the WWC is its high collection efficiency above the cutoff size, which is the minimum size particle that can be collected. For our WWC, the cutoff size was less than 1 μ m, which makes WWC suitable for collecting the hazardous bioaerosols in the respirable size range of less than 10 μm in diameter [12,33]. WWC can accommodate high air flow rates of more than 1000 LPM which is advantageous from sample collection stand point. The thin film of collection buffer, phosphate buffered saline (PBS), on the cyclone wall reduces particle bounce for continuous capture and transition of the particles into the liquid collection buffer, or hydrosol, which is directly amenable to our sensor analytical function. Particulate-containing hydrosol then flows into a sample collection reservoir.

We assessed the performance of the cyclone using a number of metrics, including the fluid recovery and collection efficiency. The fluid recovery η_r is the ratio of the collected liquid to the inputted liquid. Collection efficiency η_c is the proportion of particles captured from the aerosol by the hydrosol. These terms may be written as

$$\eta_r\,(\%) = \frac{\text{volume of fluid collected}}{\text{volume of fluid introduced}} = \frac{Q_{l,out}}{Q_{l,in}} \times 100\% \tag{1}$$

$$\eta_c\,(\%) = \frac{\text{number of particle collected}}{\text{number of particle introduced}} = \frac{c_{l,out}Q_{l,out}}{c_{a,in}Q_{a,in}} \times 100\% \tag{2}$$

where Q values are volumetric flow rates, with $Q_{a,in}$ and $Q_{l,in}$ being the air and liquid intake, respectively and $Q_{l,out}$ the liquid outflow. The c values are the concentration of particles, with $c_{a,in}$ the concentration in the air intake, and $c_{l,out}$ the concentration in the liquid outflow. The ratio between these two concentrations is a useful quantity called the concentration factor (CF). A higher CF correlates with a lower detection limit for the system. In the experiments, the air flow rate was $Q_{a,in}$ = 1200 LPM and the water flow rate was $Q_{l,in}$ = 5 mLPM. Lastly, to ensure dynamic similarity between experiments and simulations, we consider the Stokes number,

$$\text{Stk} = \frac{\text{particle response time}}{\text{fluid time scale}} = \frac{\rho_p D_p^2 U}{18\mu L} \tag{3}$$

where D_p is the particle size, ρ_p the particle density, and μ the air dynamic viscosity.

We designed a recirculation system in the WWC to recirculate the hydrosol from the sample collection reservoir back to the input spray nozzles. This process has the ability to both concentrate target particles within the hydrosol, but also decrease the amount of collection buffer needed on hand to sustain operations [34]. The system can switch between non-recirculation and circulation modes through the use of 3-way inert isolation valves (Takasago WTB-3). The system was programmed and controlled by LabView and connected to a Numato 32-Channel USB GPIO Module. In each experiment, the system was operated in non-recirculation mode for 8 min, followed by 3 min of

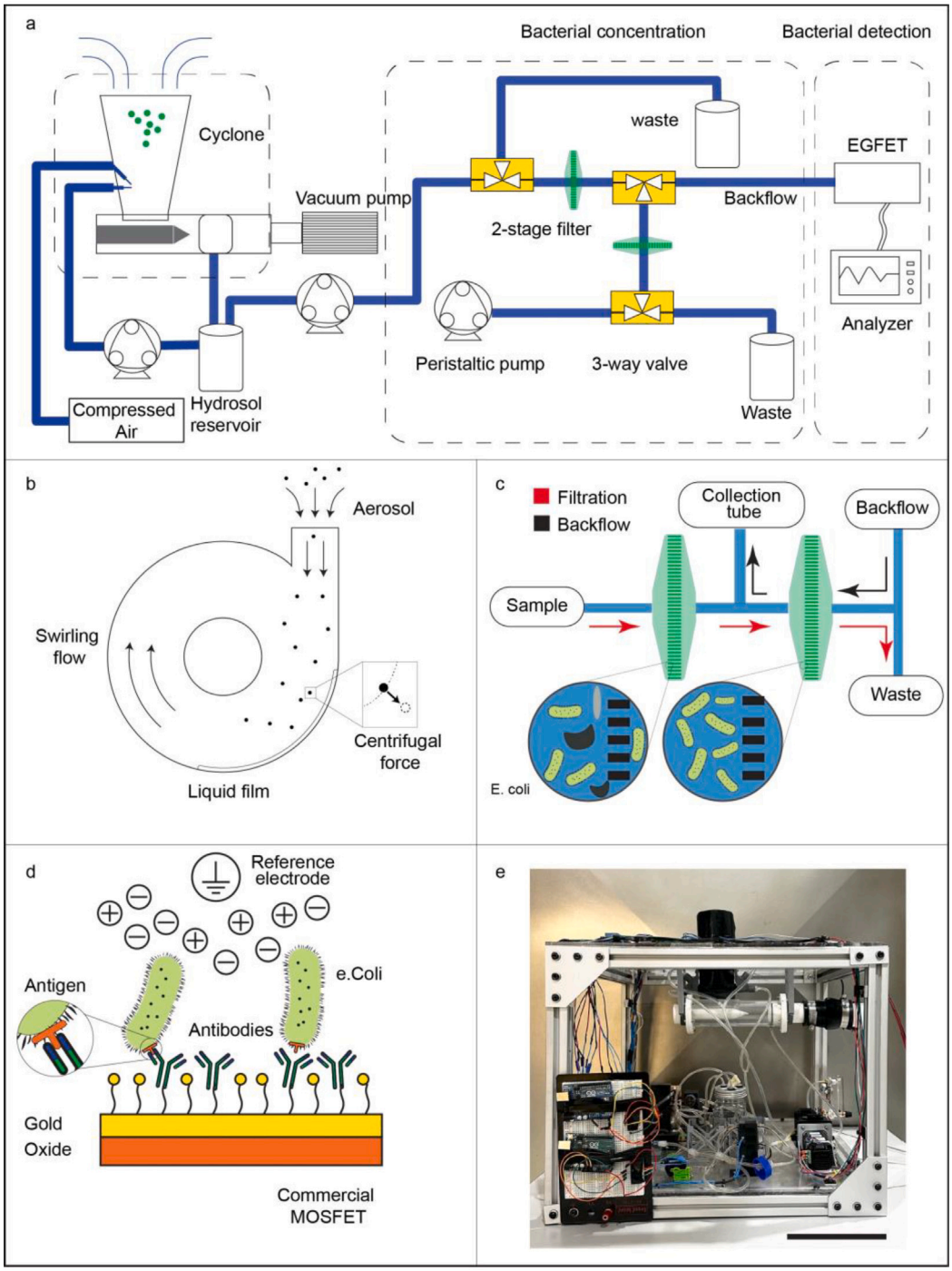

Fig. 1. (a) Schematic of our combined system for aerosol collection, filtration, and identification. The system consists of three stages, (b) aerosol collection by wet-walled cyclone, (c) concentration using a microfluidics network, and (d) detection by EGFET sensor. (e) The integrated device was used in automated fashion except for a manual transfer of analyte to the sensor (scale bar 20 cm).

recirculation and an additional 1 min of flushing to remove residual aerosols. To minimize cross-contamination between trials, the wetted wall cyclone was then cleaned by flushing with 70% ethanol for 10 min to remove residual bacteria, followed by sterile distilled water for 10 min.

2.2. Particle concentration

The microfluidics system is an optimization of the previously reported aDARE system [32]. This dual-filter (MilliporeSigma PVDF syringe filters) microfluidic system consists of two filter stages. In the first stage, a 5 μm pore filter removes particles larger than the cylindrical, approximately 1 μm × 2 μm *E. coli* followed by the second stage where a 0.22 μm pore filter captures the *E. coli* and removes the smaller particles. Eliminating non-target particulate reduces sensor background interference. The small pore filtration step also results in the loss of hydrosol volume, which beneficially increases target concentration for increased sensor sensitivity. Lastly, an optimized backflow volume flushes the *E. coli* from the small pore filter to the sensor.

Once the cyclone collects the aerosol and transfers the resulting hydrosol to the microfluidics system, 10 mL of the sample was cycled to traverse the first and second filters. Details in the valve sequence are

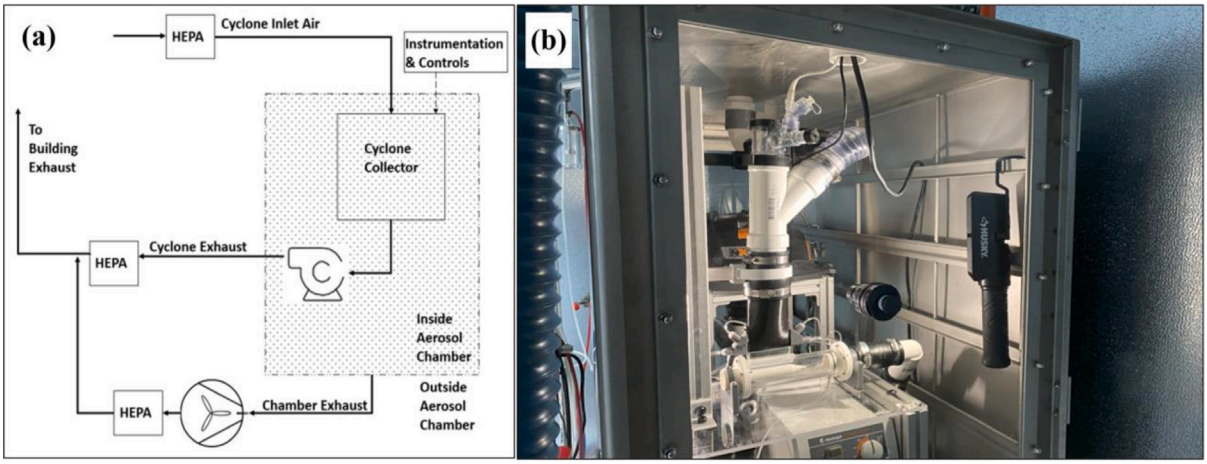

Fig. 2. (a) Airflow of cyclone in the aerosol testing chamber. Air enters the chamber after moving through an inlet HEPA filter. After exiting the chamber, air moves through another HEPA filter and meets with the chamber exhaust air, which maintains the chamber at a pressure slightly below ambient. (b) The sealed aerosol chamber containing the wet-walled cyclone.

illustrated in Supplementary Figure S1. The microfluidic system was powered by the peristaltic pumps (Clark Solutions 9QX and 15QQ) and a flow rate of 2 mL per minute was monitored by the liquid flow sensor (Sensirion SLF3S-0600F) and a microcontroller (Arduino Uno).

Similar to the definition in cyclone collection, the ratio between the input and output concentrations defines the concentration factor of the microfluidic system. Microfluidic recovery is defined below while the number of particles was determined by multiplying the concentration by the liquid volume.

$$\text{Microfluidics Recovery (\%)} = \frac{\text{number of particles in output}}{\text{number of particles in input}} \times 100\% \tag{4}$$

2.3. Particle detection

We employ an extended-gate field-effect transistor (EGFET) for particle detection. For the purposes of the prototype, the EGFET sensor was not directly integrated into the fluidics system for direct sample sensing. Instead, following collection, these samples were air-gap tested on (manually transferred to) the EGFET sensor conjugated with capture antibodies specific for *E. coli* (goat polyclonal anti-*E. coli* IgG antibodies, PA173032, Life Technologies Corp). The details of preparing and operating the conjugated sensor surface are provided under the Sensor Biomolecular Functionalization section in the supplementary information. Target capture is detected by the potentiometric change generated by the presence of charged biomolecules [35]. This change in the electric field on a surface is detected by a metal–oxide–semiconductor field effect transistor (MOSFET) electrically connected to the biochemically-sensitive surface [36,37]. Selective antibodies, negative controls, and microscope imaging provide evidence that the potentiometric change is due to the binding of the desired *E. coli* target. An EGFET refers to the complete potentiometric system, composed of the biofunctionalized surface electrically connected to the MOSFET along with a device to measure current and potential. When an external electric field is applied at the gate of the MOSFET, the current across the MOSFET changes for a given drain voltage [38].

During operation, a voltage sweep is performed before and after analyte attachment in order to measure the voltage necessary to generate a specified current. Experiments are performed in a Faraday cage, and thus any difference in the potential required to generate the same current in the MOSFET is attributed to the attached biomolecules. We call this potential difference the surface potential shift. Additionally, within the operating range of a MOSFET, the current change is correlated with the concentration of the charged biomolecules attached to the surface. Thus, a concentration-dependent response can be achieved such that a higher number of captured biomolecules results in a larger surface potential shift [39]. By performing multiple measurements, the surface potential shift can be calibrated against analyte concentration to establish pathogen threshold alert parameters.

3. Results

3.1. Cyclone efficiency

Before performing experiments with bioaerosols like *E. coli*, we first established that our cyclone could efficiently collect particles in that size range. The ability of the system to collect aerosols can be inferred from several parameters, including collection efficiency curves, cutoff size, and fluid recovery.

We benchmarked our WWC experiments to simulation and previous experiments by McFarland [12]. Fig. 3 shows the collection efficiency of the cyclone for various-sized Polystyrene Latex (PSL) fluorescent beads spanning from 0.1 to 10 μm. Our experiments are the points in blue, the experiments from McFarland et al. [12] in red, and our COMSOL simulations in black. All results show a sigmoid curve, as expected since larger particles have greater inertia and are more easily entrained by the spinning cyclone. The maximum efficiency from our experiments was 64.2% and 61.6% for the particle sizes 2.3 and 4.8 μm, respectively. Our efficiencies are less than McFarland's experiments (85%–90%) and simulation (100%). Possible reasons for the reduced efficiency are described in the discussion section.

Cutoff size D_c is defined as the particle size at which the collection efficiency η_c reaches 50%. Our experiments showed that the cutoff size for our system was 1.0 - 2.3 μm. Linear interpolation gives a cutoff size of 1.79 μm, comparable to McFarland's 1.43 μm. The simulation efficiency was higher than experimental values for all particle sizes. Consequently, the cutoff size for simulation was 1.10 μm. The experimental and simulated cutoff Stokes number was found to be 0.08 and 0.03, respectively, using the corresponding Cunningham's correction factor of 1.09 [40,41]. This implies that the particle response time is 10 to 30 times the fluid response time, indicating that particles in our experiment follow the air's streamlines. Fluid recovery indicates the system's ability to collect the inputted fluid. Fluid recovery across all trials was 79.1 ± 7.5%, resulting in a concentration factor of approximately 100,000 for PSL beads. Note that McFarland et al. reported a higher concentration factor of 780,000 at an air flow rate of 1250 LPM with *Bacillus atrophaeus* Spores [12].

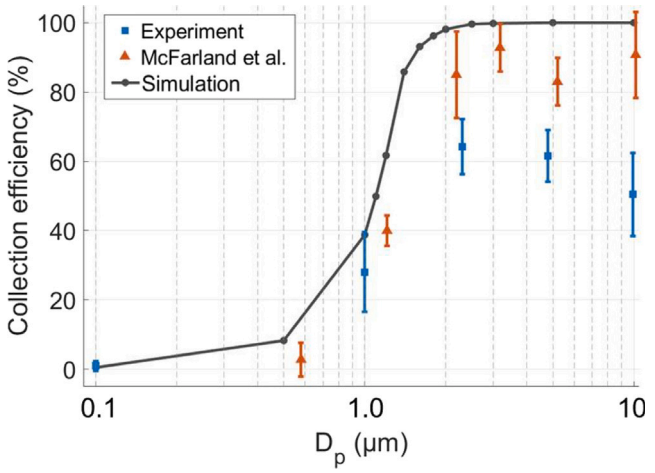

Fig. 3. Relationship between collection efficiency and particle size D_p. Experiments using PSL beads (blue), experiments from McFarland et al. 2010 (red) [12] and simulation (black).

3.2. Recirculation

Based on our experiments, we find an empirical relation for the final concentration after recirculation, which is analogous to compound interest,

$$c_{recirc} = c_0 \cdot a^t \tag{5}$$

where c_{recirc} is the concentration after recirculation, c_0 is the initial concentration, t is the recirculation time in minutes, and a is the recirculation rate.

We conducted continuous collection and recirculation with 2.3 μm fluorescent PSL beads over 7 min. Fig. 4(a) shows the time course of PSL bead concentration. A factor of 4.65 concentration increase was achieved after 7 min of recirculation, equating to a 24.6% increase per minute ($a = 1.246$). From the fluid recovery measurement, re-atomization of the hydrosol incurs approximately 20% liquid loss during open-tube recirculation. Fig. 4(b) shows that only approximately 6% of total particles were lost after 7 min, or about 0.9% per minute, suggesting that most of the target particles were retained despite the loss of liquid. We note that the recirculation tests were conducted using PSL beads, which are not easily damaged during recirculation. However, more fragile particles such as *E. coli* may undergo lysis during re-atomization, which would reduce collection efficiency of live cells.

We modified our method of recirculation for *E. coli* experiments. During a 12 min collection cycle, fresh collection liquid was introduced for the first 8 min, followed by 4 min of recirculation (3 min with aerosol introduction and 1 min without). At a liquid flow rate of 5 mL/min and 80% recovery, operating without recirculation would yield approximately 48 mL of hydrosol, which exceeds the volume needed for downstream processing. In contrast, the recirculation strategy delivers a more concentrated sample of approximately 10 mL to the microfluidics while retaining a final hydrosol volume of 20 mL for downstream analysis. We therefore adopted an 8 min fresh collection phase followed by 4 min of recirculation to balance recovery and concentration efficiency. Based on the concentration factor due to recirculation, shown in Eq. ((5)) and Fig. 4(a), we expect that our 4 min recirculation period for *E. coli* would result in a 2.4 times enhancement in the concentration.

3.3. Microfluidics optimization

We used two-stage filtration microfluidics to both concentrate the *E. coli* and remove larger particles. The volume of the backflow used to retain the bacteria from the 0.22 μm filter plays a crucial role in determining the ultimate concentration of bacteria circulating through the EGFET sensor. Insufficient backflow volume fails to recover a portion of the captured bacteria, while excessive backflow dilutes the retrieved sample. Thus, an experiment was designed to evaluate the recovery curve and determine the optimal volume for the subsequent experiments.

In these experiments, a 10 mL volume of 10^9 CFU/mL of *E. coli* was first introduced into the filtration system. While the fluid passed through the 5 μm and the 0.22 μm filters, the particles of interest are captured at the 0.22 μm filter. Next, a backflow of hydrosol transports the analyte from the filter to the sensor. To identify the optimal volume, small backflow increments of 0.3 mL were infused into different collection tubes. The output of each individual tube was plated on Tryptic Soy Agar (TSA) plates and incubated at 37 °C for 24 h to calculate the bacteria concentration. This sequential infusion facilitated the post-processing of each sample, allowing for the analysis of the correlation between the backflow volume and the corresponding retrieved bacteria. Equation (5) was used to calculate the recovery percentage for both the individual tubes and the cumulative behavior.

Fig. 5 shows the relationship between the concentration factor and recovery percentage with respect to the backflow volume. The blue curve shows the individual data from each vial, corresponding to one of 7 backflow volumes. The orange curve gives the cumulative backflow results starting from the smallest backflow volume used, 0.3 mL. There were no particles until the backflow volume of 0.4 mL, primarily due to the priming of the tubes. The backflow at 0.9 mL produces a high concentration factor, but it recovers less than 40% of the captured bacteria. Successive backflows show a plateau in bacteria recovery of 85% after infusing 3 mL. Further increases in backflow volume yield diminishing returns in recovery. The cumulative concentration factor peaks at 2.5 for the 3 mL backflow volume, leading us to establish 3 mL as the optimized backflow volume for our study.

3.4. EGFET testing

Surface plasmon resonance (SPR) experiments were performed to validate the chosen antibody and surface functionalization procedure for target *E. coli* selectivity. SPR was chosen for its ability to sense mass attachment to a surface in real-time while evaluating antibody binding efficacy [42]. These tests used the same *E. coli* strain to validate sensor output and optimize process conditions. Fig. 6(a) shows the SPR response of the selected *E. coli*-specific antibody compared to an isotype control antibody (goat IgG control, #026202, Life Technologies Corp) for three different bacteria concentrations. An isotype control antibody experiment was included to confirm that the receptor antibody bound *E. coli* via selective affinity.

In Fig. 6(a), the signal is generated by subtracting the SPR response of the active channel containing the E. coli-specific antibodies from the response of the control channel, which contains IgG control antibodies. Each antibody was tested using its own active and control channel. The difference in response is attributed to the attachment of *E. coli* cells to the antibody. The results are expressed cumulatively as higher concentrations of *E. coli* solution are applied to the surface. As expected, the response from the channel containing the anti-*E. coli* antibodies increases as bacteria concentration increases from 10^6 CFU/mL to 10^8 CFU/mL. In comparison, the isotype control antibodies experience a net decrease. A negative response is recorded by the isotype control antibody due to higher binding on the control channel, which contains no antibody, than the active.

In addition to SPR testing, we validated that the biofunctionalized surface used on the EGFET can capture *E. coli* cells from solution and that this alters the surface potential. We exposed a control and active sensor channel to the same bacteria solution and measured the potential change. The control channel is an unmodified SAM (self-assembled monolayer), while the active channel is functionalized with antibodies. More details for the functionalization and operating process

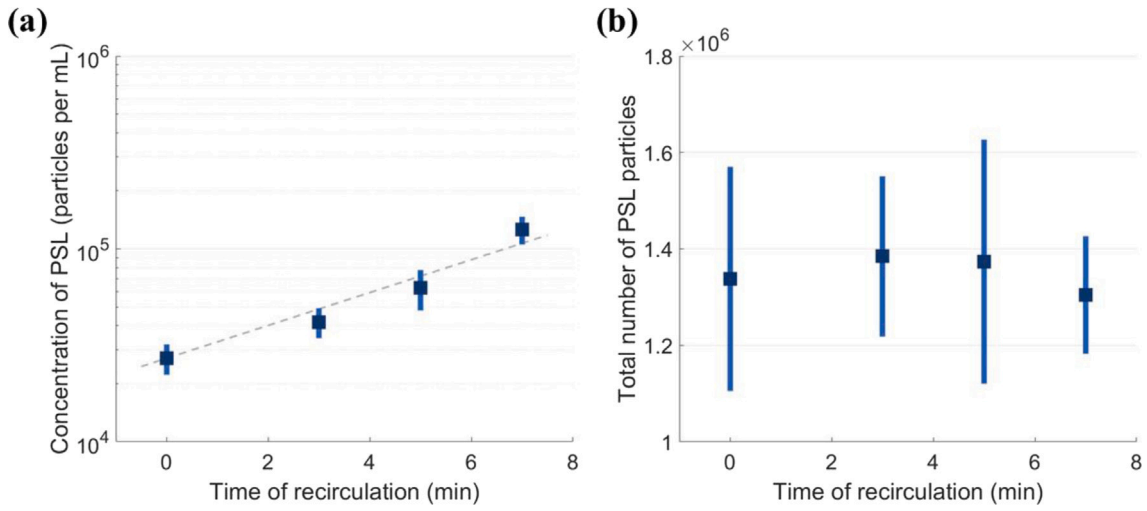

Fig. 4. Cyclone recirculation results using PSL beads. (a) Relationship between particle concentration and time of recirculation along with fitted line based on Eq. (5) (dashed). Concentration increased by a factor of 4.7 over 7 min. (b) Relationship between estimated total number of particles and time of recirculation which only 6% loss occurred over 7 min.

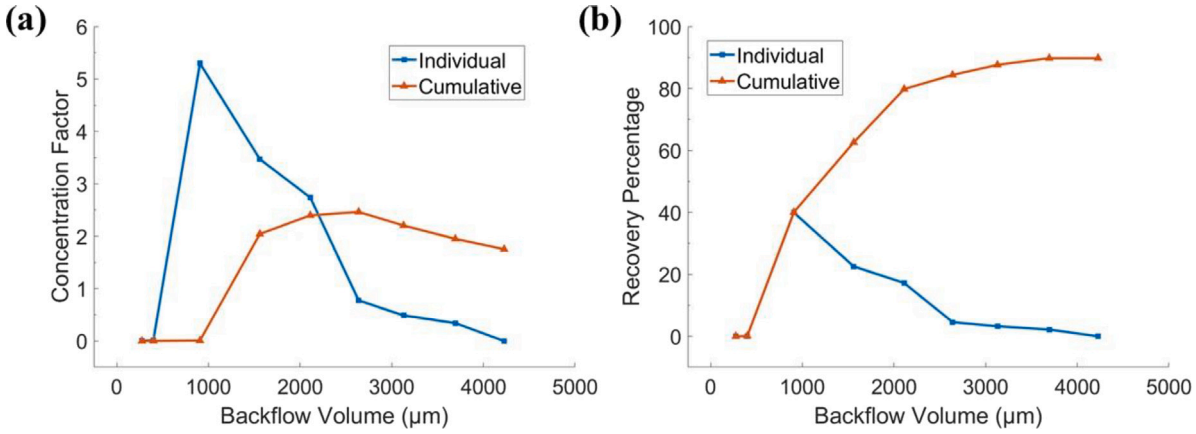

Fig. 5. (a) Relationship between concentration factor and backflow volume. (b) Relationship between recovery percentage and backflow volume. Individual vials (blue) and cumulative volume (red)

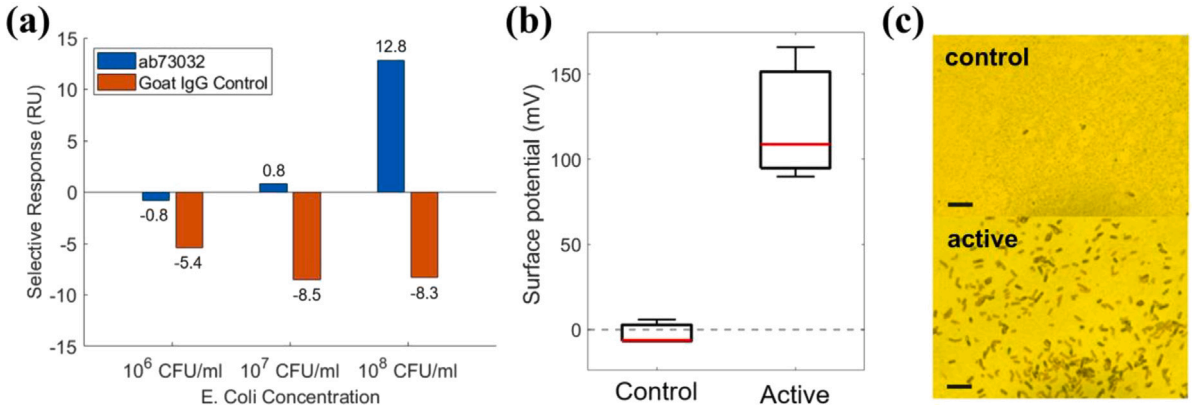

Fig. 6. (a) SPR binding response comparing ab73032 and isotype control. (b) Biofunctionalized surface potential shift observed in the presence of *E. coli*, at a concentration of 10^8 CFU/mL. Active and control channels refer to a surface with and without *E. coli* antibodies. (c) Microscopic views of the samples showing *E. coli* attachment. Scale bars, 10 μm).

are provided under Sensor Biomolecular Functionalization within the supplementary information. To independently confirm that the surface potential changes when *E. coli* is adhered, we directly measured the potential change of the chip before and after bacteria exposure. The surface potential was measured directly by the Keithley 4200 SCS without integrating the MOSFET. Fig. 6(b) shows a 121.5 mV surface potential shift produced by the active sensors at concentration 10^8 CFU/mL, while the control sensors, as expected, show a negligible

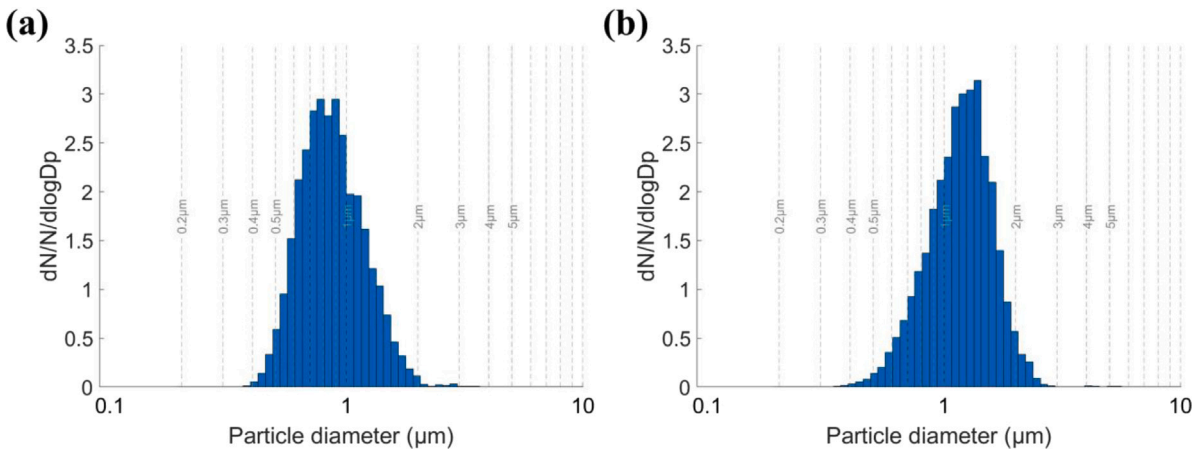

Fig. 7. Histogram of aerosol size distribution, where N is the total number of particles and dN is the number of particles within a given size range. The vertical axis is normalized by the logarithmic bin width $d\log D_p$, (a) Pure saline. (b) *E. coli* culture, which contains 4.4×10^7 CFU per mL of culture. The addition of *E. coli* shifts the peak to the right near the bacterial size, suggesting bioaerosol generation was effective.

surface potential shift of −2.5 mV. Moreover, the microscope images in Fig. 6(c) confirm that the active sensors captured *E. coli* cells while the control sensors did not.

3.5. Aerosol chamber E. coli test

Before testing the integrated system, we analyzed the particle distribution from our aerosolized *E. coli* solution. Fig. 7 depicts the aerosol size distribution for 10^5 CFU/mL *E. coli* solution compared to pure saline. We observed the presence of *E. coli*, as shown by the change in peak particles from 0.5-1.0 μm for saline to 1-2 μm for *E. coli*. This latter size range is comparable to the characteristic size of *E. coli*, which is 1 μm in diameter and 2 μm in length. Other features that may improve the capture of *E. coli* in our WWC are its greater density than water: each unit has a mass close to 1 pg (picogram) and a density about 1.3 times greater than water [43–45]. The *E. coli* aerosols generation and collection experiments described here took place inside an aerosol containment chamber (Customized Biosensor Testing System, CH Technologies, Westwood, NJ) with ambient air circulated through HEPA filtration, as shown in Fig. 2.

3.6. Tests of integrated system with E. coli

We performed testing of the integrated collection and fluidics system under three conditions, each in triplicate for a total of 9 trials. The conditions include nebulizing a control buffer with no bacteria, or with two concentrations (5×10^3 CFU/mL and 1×10^4 CFU/mL). Note that throughout our study, we measured concentration using plating; thus we only report live bacteria particles. The number of dead particles too can be read by the EGFET, but their change in concentration was not measured in this study.

Each sample was aerosolized for 11 min, in which the wetted wall cyclone performed an 8 min normal collection phase followed by a 3 min collection in the hydrosol recirculation phase. After aerosolization was complete, the cyclone continued operating for an additional minute to clean up residual aerosols and collection liquid still within the system.

After collection, the integrated microfluidic system processed 10 mL of the collected hydrosol at a rate of 2 mL/min and after-filter backwash delivered 3.13 ± 0.34 mL and 2.98 ± 0.14 mL for the two concentrations of *E. coli*, respectively, to the EGFET module in under 8 min. For the control case using pure PBS, the system delivered 2.71 ± 0.05 mL of hydrosol. A total of 27 measurements were taken, three samples of each concentration were provided with each sample being tested on three independent electrodes. However, the first three measurements produced for the high concentration (1×10^4 CFU/mL) had to be discarded due to a failure of the commercial MOSFET.

The EGFET results are provided in Fig. 8(a). As expected, the control response provides the lowest magnitude surface potential shift. Increasing concentrations of *E. coli* produced a higher magnitude response, with the bacterial concentration of 5×10^3 CFU/mL achieving a 64 ± 36 mV and the concentration of 1×10^4 CFU/mL achieving a 165 ± 73 mV. The concentration of the feeding air was calculated based on the atomizer's consumption of the input sample and the cyclone's air intake rate. The resulting concentrations $c_{a,in}$ were 7.7 CFU/L and 15.4 CFU/L for the two *E. coli* input levels, respectively.

We proceeded by determining the increases in concentration of bacteria at each stage of the system. We sampled 50 μL from each collected hydrosol for CFU quantification. Fig. 8(b) illustrates the bacteria count measurements for the three stages. Upon the cyclone collection and recirculation, the bacterial concentration increased by 8.4 and 4.0 times from the initial solution for two initial concentrations, respectively. The microfluidics system further concentrated by 2.7 and 1.9 times, resulting in overall liquid-to-liquid concentration factors of 22.8 and 7.8 for two concentrations. The final analyte concentrations $c_{l,out}$ delivered to the sensor were 1.26×10^5 CFU/mL and 1.13×10^5 CFU/mL, respectively. Based on the corresponding feeding air concentrations (7.7×10^{-3} CFU/mL and 15.4×10^{-3} CFU/mL), the overall air-to-liquid concentration factors became 16,400,000 and 7,300,000, respectively.

4. Discussion

4.1. Individual module performance

Our wetted wall cyclone design consistently underperformed for large particles (above 2.3 μm) in comparison to McFarland's cyclone [12] and our simulations. This is presumably due to our higher liquid flow rates of 5 mLPM, which is five times higher than McFarland's work. McFarland stated that increased liquid flow rates may adversely affect the cyclone's collection efficiency. Another reason for underperformance may be our method of aerosolizing PSL beads. We hypothesize that some collected aerosol volume failed to completely enter the collection system. In fact, during testing, we observed residual aerosol solution adhering to the corrugated hose connecting the vacuum source, particularly at bends in the pathway. Future work could replace the corrugated hose with a smooth hose to minimize dead zones for input aerosols. Moreover, fluorescence-based quantification of PSL beads may introduce bias, as larger beads tend to sediment during measurement and can yield lower apparent signal intensity.

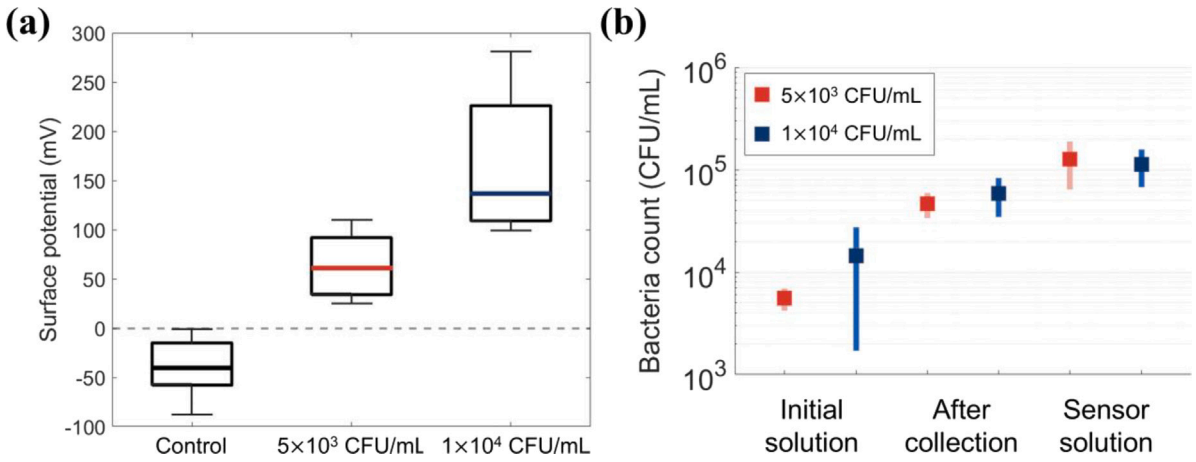

Fig. 8. Demonstration of *E. coli* detection using integrated system with EGFET. (a) Surface potential shift for three experimental conditions (control, two concentrations of bacteria). Concentrations indicate the initial solution conditions before aerosolization. (b) The bacteria count from culturing samples extracted at each stage of the pipeline for our integrated device.

While the 0.22 μm filter of the microfluidics can be susceptible to clogging in contaminated samples, the 5 μm filter functions as a pre-filter by removing larger particulates that contribute to blockage. The selection of the 5 μm filter was supported by prior work [46], where it was demonstrated to effectively reduce interfering particles. In environments with a high contaminant burden, the system can be readily adapted to incorporate a cascade of filters with graded pore sizes to enhance reliability and performance. In this study, an external HEPA filter was employed as an additional pre-filter. In the absence of this filter, we hypothesize that the 5 μm filter would experience an increased filtration load, but the system should still collect target particles as designed.

As an electrochemical sensor conjugated to target-specific antibodies, the EGFET represents the fastest technique because it detects target pathogen in its native form without sample processing or preparation. The microfluidic system was optimized to provide sufficient concentration and volume of the *E. coli* sample for EGFET. The procedures may be adjusted for the different collection configurations and target particle detection applications. This study assumed that *E. coli* viability is not lost during the aerosolization, collection, and analysis studies. However, loss of viability may not immediately affect an organism's structure or its ability to bind to sensor antibodies. Future studies could explore the potential loss of viability of collected pathogens at each stage of the process. Also, aerosolized *E. coli* droplets in our experiments may differ from the complex biological composition of airborne particulates expelled from human lungs. Developing artificial bioaerosols that better simulate real-life conditions could be a valuable direction for future work. For sub-micron sized viral particle targets too small for pore capture, a tangential flow filtration device could replace the small pore filter [47].

During preliminary testing, the surface potential was directly tested using the Keithley 4200 SCS. In contrast, during integration testing, the full EGFET device, including the n-channel MOSFET, was utilized to process the signal before reading with the Keithley device. The goal is that future tests can replace the Keithley due to its high cost, and the use of a MOSFET is conducive to a cheaper design. Many alternative source measurement units (SMU's) offer a different balance of cost, size, and sensitivity depending on project needs. For example, a more accessible option is the Analog Discovery 3 with the Transistor Tester add-on (Digilent, Austin, TX). For further details on MOSFET operation, Kar provides an excellent resource on operational basics [48].

The selectivity of our sensor is a function of the specificity of the associated bioreceptor. Thus, by switching out the bioreceptor, this technology may be extended to detect any pathogen with a known bioreceptor. Further, by adding additional, parallel sensor channels, this technology could easily be multiplexed for many different pathogens.

4.2. Context of integrated device performance

To apply our device in different contexts, such as heating, ventilation, and air conditioning (HVAC), we calculate several key properties of the aerosolized bacterial solution. Using these values, we can benchmark our experiments against previous studies. Our study was motivated by studying high volumetric flow rates of air, which will have lower airborne pathogen concentrations. We focus our calculations on the lower of the two *E. coli* concentrations studied here, which was $c = 5{\times}10^3$ CFU/mL. Approximately 20 mL of this sample was nebulized during the experiment ($V = 20$ mL), resulting in $n = cV = 1 \times 10^5$ CFU of bacteria aerosolized.

Given the operation time T and air flow rate Q, the concentration of the bacteria in the air $c_a = n/QT = 7.7$ CFU/L. In nature, this is a low concentration: in comparison, aerodynamic particle sizers have measured absolute numbers of particles, like aerosolized *Bacillus globigii* spores at 160 particles per liter of air [49]. While we were aiming for high air flow rate and low bacteria concentration, we find the concentration captured is mid-range compared to currently available systems. For instance, a system using impactors and filters achieved a filter-based collection of *M. smegmatis* at concentrations ranging from 0.2 to 22 CFU per liter of air [50]. Another study using a smaller wet cyclone managed to collect *S. epidermidis* at a concentration of 200 CFU/L of air [22].

Another limitation of our current cyclone design is that the hydrosol is recirculated through open tubing, which can lead to evaporation and reduce liquid recovery. In our tests, this effect contributed to approximately 20% liquid loss, though particle counts remained largely preserved. While this did not significantly bias our concentration factor estimates, future iterations of the system will incorporate sealed or minimized recirculation pathways to mitigate evaporation and improve sampling accuracy. Although the wetted wall cyclone is effective for high-volume collection, its geometry can make thorough cleaning between experiments challenging. We addressed this by instituting a standardized cleaning protocol of ethanol flush followed by sterile water rinsing. While this minimized the risk of cross-contamination in the present study, future iterations of the system could benefit from design modifications that facilitate easier cleaning and maintenance for long-term or continuous operation.

E. coli was detected in air samples with concentrations as low as 7.6 CFU/L. This demonstrates operational success in relatively low live bacteria concentration aerosols. The EGFET with antibody receptors is expected to bind both live and dead *E. coli* cells, providing broad sensing flexibility. Our study reports cellular concentration in terms of CFU/L as we used plating to determine analyte concentration. Thus,

the use of CFU/L serves as a limitation in this work as it only measures the live cells. Previous researchers have differentiated live and dead bacteria using microfluidic cytometry [29] and use of this technology may help preserve the integrity of collected samples. Future work exploring our technique while differentiating live and dead cells would be of use to the research community.

Our study demonstrates the cellular detection of *E. coli* as a model system. We had intended the system to work in an integrated fashion but ultimately we performed a manual transfer to the sensor. Future sensor technologies may make the sensing more reliable. For example, a potentiometric transducer utilizes an immunosensor receptor layer to differentiate *E. coli* when present in solution. By using antibody receptors, it is expected that this proof of concept sensor can easily be scaled to many other bacteria or viruses simply by changing the antibody. Immunosensors are well established in the literature for the breadth of application and potential for multiplexing [51].

Our prototype was designed with the goal of integration into an indoor HVAC system. Our technology also holds the potential for miniaturization in terms of size, weight, and power (SWaP). Such advancements could enable deployment as a robot or drone payload for application for environmental pathogen detection in agriculture settings for plant and animal health and for military biodefense capabilities.

5. Conclusion

We combined a wetted wall cyclone with microfluidics and EGFET sensor to detect the capture of *E. coli* aerosols. We designed and introduced a novel recirculation system for use in increasing the particle concentration in the cyclone. The cyclone collection was over 60% efficient for PSL beads near 2 μm. Our system achieves a detection of 7.7 CFU per liter of air with an EGFET surface potential shift of 64 ± 36 mV over a 12 min collection phase and following an 8 min concentration and 30 min detection phase. Our prototype for detection of airborne pathogens may have use in both public health and agricultural environmental monitoring.

CRediT authorship contribution statement

Soohwan Kim: Writing – review & editing, Writing – original draft, Visualization, Methodology, Investigation, Formal analysis, Data curation. **Noah Baughman:** Writing – review & editing, Writing – original draft, Methodology, Formal analysis, Data curation. **Mohamed Badawy:** Writing – original draft, Methodology, Formal analysis, Data curation. **Margaret Armstrong:** Software, Resources, Methodology. **Kristina Wayne:** Software, Methodology. **Eric Vogel:** Supervision, Resources, Funding acquisition. **Craig R. Forest:** Supervision, Resources, Funding acquisition. **David L. Hu:** Writing – review & editing, Supervision, Resources, Project administration, Funding acquisition. **Michael L. Farrell:** Writing – review & editing, Supervision, Resources, Project administration, Funding acquisition.

Declaration of competing interest

The authors declare the following financial interests/personal relationships which may be considered as potential competing interests: Michael Farrell reports financial support was provided by Georgia Institute of Technology Research Institute. Michael Farrell reports financial support was provided by Defense Advanced Research Projects Agency. Michael Farrell, David Hu, Soohwan Kim has patent #8903: Recirculation System for Aerosol Collectors Maximizes Particle Concentration for Improved Pathogen Detection issued to Georgia Tech Office of Technology Licensing. If there are other authors, they declare that they have no known competing financial interests or personal relationships that could have appeared to influence the work reported in this paper.

Acknowledgments

This research was supported by the Georgia Tech Research Institute (GTRI) IRAD program and by the DARPA SenSARS program: HR00112190060. The authors would like to thank J. Beyersdorf and P. Santangelo for their helpful discussion and insight, S. Ritchter and J. Xu for their help in preparing the bacteria for our experiments.

Appendix A. Supplementary data

Supplementary material related to this article can be found online at https://doi.org/10.1016/j.snb.2025.139037.

Data availability

Data will be made available on request.

References

[1] S. Bagcchi, Who's global tuberculosis report 2022, Lancet Microbe 4 (1) (2023) e20.
[2] J.A. Huffman, A.E. Perring, N.J. Savage, B. Clot, B. Crouzy, F. Tummon, O. Shoshanim, B. Damit, J. Schneider, V. Sivaprakasam, et al., Real-time sensing of bioaerosols: Review and current perspectives, Aerosol Sci. Technol. 54 (5) (2020) 465–495.
[3] Z. Xu, Y. Wu, F. Shen, Q. Chen, M. Tan, M. Yao, Bioaerosol science, technology, and engineering: past, present, and future, Aerosol Sci. Technol. 45 (11) (2011) 1337–1349.
[4] B.U. Lee, I.G. Hong, D.H. Lee, E.-S. Chong, J.H. Jung, J.H. Lee, H.J. Kim, I.-S. Lee, et al., Bacterial bioaerosol concentrations in public restroom environments, Aerosol Air Qual. Res. 12 (2) (2012) 251–255.
[5] C.Y. Rao, H.A. Burge, J.C. Chang, Review of quantitative standards and guidelines for fungi in indoor air, J. Air Waste Manage. Assoc. 46 (9) (1996) 899–908.
[6] G. Omelianetz, Biological hazards as risks factors in microbial industry, Pharmacol Toxicol. Suppl 80 (1997) 141–145.
[7] B. Ghosh, H. Lal, A. Srivastava, Review of bioaerosols in indoor environment with special reference to sampling, analysis and control mechanisms, Environ. Int. 85 (2015) 254–272.
[8] R. Jabeen, M.I. Kizhisseri, S. Mayanaik, M.M. Mohamed, Bioaerosol assessment in indoor and outdoor environments: a case study from India, Sci. Rep. 13 (1) (2023) 18066.
[9] E. Brągoszewska, I. Biedroń, A. Mainka, Microbiological air quality in a high-school gym located in an urban area of Southern Poland—Preliminary research, Atmosphere 11 (8) (2020) 797.
[10] J.H. Seo, H.W. Jeon, J.S. Choi, J.-R. Sohn, Prediction model for airborne microorganisms using particle number concentration as surrogate markers in hospital environment, Int. J. Environ. Res. Public Heal. 17 (19) (2020) 7237.
[11] C.P. Weis, A.J. Intrepido, A.K. Miller, P.G. Cowin, M.A. Durno, J.S. Gebhardt, R. Bull, Secondary aerosolization of viable *Bacillus anthracis* spores in a contaminated US Senate Office, Jama 288 (22) (2002) 2853–2858.
[12] A.R. McFarland, J.S. Haglund, M.D. King, S. Hu, M.S. Phull, B.W. Moncla, Y. Seo, Wetted wall cyclones for bioaerosol sampling, Aerosol Sci. Technol. 44 (4) (2010) 241–252.
[13] J. Ma, M. Du, C. Wang, X. Xie, H. Wang, Q. Zhang, Advances in airborne microorganisms detection using biosensors: A critical review, Front. Environ. Sci. Eng. 15 (2021) 1–19.
[14] J. Li, J. Macdonald, F. Von Stetten, A comprehensive summary of a decade development of the recombinase polymerase amplification, Analyst 144 (1) (2019) 31–67.
[15] J. Boreson, A.M. Dillner, J. Peccia, Correlating bioaerosol load with PM2. 5 and PM10cf concentrations: a comparison between natural desert and urban-fringe aerosols, Atmos. Environ. 38 (35) (2004) 6029–6041.
[16] M. Tan, F. Shen, M. Yao, T. Zhu, Development of an automated electrostatic sampler (AES) for bioaerosol detection, Aerosol Sci. Technol. 45 (9) (2011) 1154–1160.
[17] M. Li, L. Wang, W. Qi, Y. Liu, J. Lin, Challenges and perspectives for biosensing of bioaerosol containing pathogenic microorganisms, Micromachines 12 (7) (2021) 798.
[18] S. Hou, M. Wu, H. Li, H.-R. Gong, Z. Gao, R. Shi, X. Huang, D. Li, J.-D. Huang, J. Yu, et al., Ultrasensitive detection of SARS-CoV-2 by flexible metal oxide field-effect transistors, Adv. Funct. Mater. 33 (41) (2023) 2301268.

[19] A. Purwidyantri, H.-C. Lai, S.-H. Tsai, J.-D. Luo, C.-C. Chiou, Y.-C. Tian, C.-H. Cheng, Y.-T. Lin, C.-S. Lai, Sensing performance of fibronectin-functionalized Au-EGFET on the detection of S. epidermidis biofilm and 16S rRNA of infection-related bacteria in peritoneal dialysis, Sensors Actuators B: Chem. 217 (2015) 92–99.
[20] D.P. Greenwood, T.H. Jeys, B. Johnson, J.M. Richardson, M.P. Shatz, Optical techniques for detecting and identifying biological-warfare agents, Proc. IEEE 97 (6) (2009) 971–989.
[21] K. Kukula, D. Farmer, J. Duran, N. Majid, C. Chatterley, J. Jessing, Y. Li, Rapid detection of bacteria using raman spectroscopy and deep learning, in: 2021 IEEE 11th Annual Computing and Communication Workshop and Conference, CCWC, IEEE, 2021, pp. 0796–0799.
[22] Y.S. Cho, S.C. Hong, J. Choi, J.H. Jung, Development of an automated wet-cyclone system for rapid, continuous and enriched bioaerosol sampling and its application to real-time detection, Sensors Actuators B: Chem. 284 (2019) 525–533.
[23] Y.S. Cho, H.R. Kim, H.S. Ko, S.B. Jeong, B. Chan Kim, J.H. Jung, Continuous surveillance of bioaerosols on-site using an automated bioaerosol-monitoring system, ACS Sensors 5 (2) (2020) 395–403.
[24] A. Kaushik, S. Tiwari, R.D. Jayant, A. Marty, M. Nair, Towards detection and diagnosis of Ebola virus disease at point-of-care, Biosens. Bioelectron. 75 (2016) 254–272.
[25] P. Skládal, E. Švábenská, J. Žeravík, J. Přibyl, P. Šišková, T. Tjärnhage, I. Gustafson, Electrochemical immunosensor coupled to cyclone air sampler for detection of *Escherichia coli* DH5α in bioaerosols, Electroanalysis 24 (3) (2012) 539–546.
[26] S. Jiang, S. Qian, Y. Guo, Y. Geng, B. Guo, Z. Chen, R. Yang, X. Chen, Z. Guo, S. Liu, Integrated fiber-optic SPR sensor with cyclone sampling for rapid on-site bioaerosol pathogen detection, ACS Sensors (2025).
[27] P. Skládal, et al., Electrochemical immunosensor coupled to cyclone air sampler for detection of *Escherichia coli* DH5α in bioaerosols, Electroanalysis 24 (3) (2012) 539–546.
[28] S. Jiang, et al., Integrated fiber-optic SPR sensor with cyclone sampling for rapid on-site bioaerosol pathogen detection, ACS Sensors 10 (8) (2025) 6058–6064.
[29] C.H. Lee, H. Seok, W. Jang, J.T. Kim, G. Park, H.-U. Kim, J. Rho, T. Kim, T.D. Chung, Bioaerosol monitoring by integrating DC impedance microfluidic cytometer with wet-cyclone air sampler, Biosens. Bioelectron. 192 (2021) 113499.
[30] G.-w. Sung, C. Ahn, T. Kim, Real-time FET-based biosensor using the wet cyclone air sampler, in: Electrochemical Society Meeting Abstracts, vol. 226, (51) The Electrochemical Society, Inc., 2014, 2313–2313.
[31] J.V. Puthussery, et al., Real-time environmental surveillance of SARS-CoV-2 aerosols, Nat. Commun. 14 (1) (2023) 3692.
[32] N.S.F. Guzmán, M.W. Badawy, M.A. Stockslager, M.L. Farrell, C. van Zyl, S. Stewart, D.L. Hu, C.R. Forest, Quantitative assessment of automated purification and concentration of E. coli bacteria, SLAS Technol. (2023).
[33] M.I. Guzman, An overview of the effect of bioaerosol size in coronavirus disease 2019 transmission, Int. J. Heal. Plan. Manag. 36 (2) (2021) 257–266.
[34] M.L. Farrell, D. Hu, S. Kim, S.A. Stewart, Recirculation system for aerosol collectors using liquid collection buffer, 2025, Google Patents, US Patent App. 18/836, 286.
[35] D.R. Thévenot, K. Toth, R.A. Durst, G.S. Wilson, Electrochemical biosensors: recommended definitions and classification, Biosens. Bioelectron. 16 (1–2) (2001) 121–131.
[36] I. Lauks, P. Chan, D. Babic, et al., The extended gate chemically sensitive field effect transistor as multi-species microprobe, Sensors Actuators 4 (1983) 291–298.
[37] T. Sakata, S. Matsumoto, Y. Nakajima, Y. Miyahara, Potential behavior of biochemically modified gold electrode for extended-gate field-effect transistor, Japan. J. Appl. Phys. 44 (4S) (2005) 2860.
[38] V. Barkhordarian, et al., Power MOSFET basics, Powerconversion Intell. Motion-English Ed. 22 (6) (1996) 2–8.
[39] A. Tarasov, D.W. Gray, M.-Y. Tsai, N. Shields, A. Montrose, N. Creedon, P. Lovera, A. O'Riordan, M.H. Mooney, E.M. Vogel, A potentiometric biosensor for rapid on-site disease diagnostics, Biosens. Bioelectron. 79 (2016) 669–678.
[40] E. Cunningham, On the velocity of steady fall of spherical particles through fluid medium, Proc. R. Soc. Lond. Ser. A, Containing Pap. A Math. Phys. Character 83 (563) (1910) 357–365.
[41] C. Davies, Definitive equations for the fluid resistance of spheres, Proc. Phys. Soc. 57 (4) (1945) 259.
[42] X. Guo, Surface plasmon resonance based biosensor technique: a review, J. Biophotonics 5 (7) (2012) 483–501.
[43] R. Gilbert, Physical biology of the cell, by Rob Phillips, Jane Kondev and Julie Theriot, Taylor & Francis, 2009.
[44] F.C. Neidhardt, Escherichia coli and Salmonella: cellular and molecular biology, (579.8 ESC) 1996.
[45] J. Howard, Mechanics of motor proteins and the cytoskeleton: Sinauer assoc, 2001, Sunderland, MA.
[46] S. Isabel, M. Boissinot, I. Charlebois, C.M. Fauvel, L.-E. Shi, J.-C. Lévesque, A.T. Paquin, M. Bastien, G. Stewart, É. Leblanc, et al., Rapid filtration separation-based sample preparation method for Bacillus spores in powdery and environmental matrices, Appl. Environ. Microbiol. 78 (5) (2012) 1505–1512.
[47] P. Agrawal, K. Wilkstein, E. Guinn, M. Mason, C.I. Serrano Martinez, J. Saylae, A review of tangential flow filtration: process development and applications in the pharmaceutical industry, Org. Process. Res. Dev. 27 (4) (2023) 571–591.
[48] S. Kar, Mosfet: Basics, characteristics, and characterization, in: High Permittivity Gate Dielectric Materials, Springer, 2013, pp. 47–152.
[49] M. Dybwad, G. Skogan, J.M. Blatny, Comparative testing and evaluation of nine different air samplers: end-to-end sampling efficiencies as specific performance measurements for bioaerosol applications, Aerosol Sci. Technol. 48 (3) (2014) 282–295.
[50] R. Wood, C. Morrow, C.E. Barry III, W.A. Bryden, C.J. Call, A.J. Hickey, C.E. Rodes, T.J. Scriba, J. Blackburn, C. Issarow, et al., Real-time investigation of tuberculosis transmission: developing the respiratory aerosol sampling chamber (RASC), PloS One 11 (1) (2016) e0146658.
[51] A. Jones, et al., Multiplexed immunosensors and immunoarrays, Anal. Chem. 92 (1) (2019) 345–362.

Soohwan Kim is a doctoral student in Mechanical Engineering at the Georgia Institute of Technology. His research focuses on aerosol collection, fluid simulation, and bio-inspired fluid phenomena.

Noah Baughman is a doctoral student in Materials Science and Engineering at the Georgia Institute of Technology. His research focuses on electrochemical biosensing, surface engineering, and semiconductor fabrication.

Mohamed Badawy is a doctoral student in Mechanical Engineering at the Georgia Institute of Technology. He holds an M.Sc. in Mechanical Engineering from Cairo University. His research focuses on paper-based microfluidics and the development of rapid diagnostic assays.

Margaret Armstrong is a Research Engineer at Georgia Tech Research Institute. She received her degrees in mechanical engineering from Georgia Institute of Technology. Her research focuses on rapid prototyping of concepts for ground maneuver forces.

Kristina Wayne is a Research Engineer at the Georgia Tech Research Institute. She received her degrees in mechanical engineering and applied systems engineering from the Georgia Institute of Technology. Her work focuses on rapid prototyping and modeling, simulation, and analysis.

Eric M. Vogel is a Professor in the School of Materials Science and Engineering at the Georgia Institute of Technology and the Executive Director of the Georgia Tech Institute for Matter and Systems. He received his Ph.D. in Electrical Engineering from North Carolina State University. His research focuses on neuromorphic devices, nanoelectronic materials, and biosensors.

Craig R. Forest is a Professor of Mechanical Engineering at the Georgia Institute of Technology and a founding member of the NSF Center for Cell Manufacturing Technologies (CMaT). He received his Ph.D. in Mechanical Engineering from MIT. His research integrates microsystems, automation, and biological experimentation, with applications in diagnostics, neuroscience, and cell manufacturing.

David Hu is a Professor of Mechanical Engineering and Biology, and an Adjunct Professor of Physics at the Georgia Institute of Technology. He received his degrees in mathematics and mechanical engineering from the Massachusetts Institute of Technology. His research interests span biomechanics, fluid dynamics, and animal locomotion.

Michael L. Farrell is a Principal Research Scientist at the Georgia Tech Research Institute and Adjunct Faculty in the School of Biological Sciences at Georgia Tech. He received his Ph.D. in Virology from the University of Wisconsin– Madison. His research focuses on developing low-cost, field-deployable biosensing technologies and high-volume pathogen collection systems.